

Theory of carbon-carbon pairs in silicon

R. B. Capaz

Instituto de Física, Universidade Federal do Rio de Janeiro, Caixa Postal 68528, Rio de Janeiro, RJ 21945-970, Brazil

A. Dal Pino, Jr.

Instituto Tecnológico de Aeronáutica, São José dos Campos, SP 12225, Brazil

J. D. Joannopoulos

Department of Physics, Massachusetts Institute of Technology, Cambridge, Massachusetts 02139

(Received 19 March 1998)

Interstitial-substitutional carbon pairs (C_iC_s) in silicon display interesting metastable behavior associated with two different structural configurations. In this work, we perform extensive *ab initio* calculations on this system. Our results show the following. (i) The metastable configuration for the neutral charge state displays C_{1h} symmetry and it is reminiscent of the isolated interstitial carbon configuration, i.e., a split interstitial C-Si pair with the substitutional carbon bonded to the silicon interstitial. (ii) The ground-state configuration also has C_{1h} symmetry, but it consists of a single silicon interstitial twofold coordinated in an unusual bridge configuration between two substitutional carbon atoms. With an activation energy of 0.07 eV, this configuration becomes a motional-averaged state with C_{3v} symmetry. (iii) The ground state is lower in energy by 0.11 eV with respect to the metastable state. The jump from one configuration to the other corresponds to a simple “bond-switching” mechanism with a calculated energy barrier of 0.13 eV. (iv) Both configurations have two electronic states in the gap, with gap-state wave functions consistent with the local bonding of the defect complex in each case. (v) Analysis of local-mode vibrations on the ground-state configuration indicates a stronger component in one of the carbon atoms, which explains the experimentally observed isotope splittings. Vibrational frequencies for the metastable configuration are also predicted. All of these results are in satisfactory agreement with experiments. [S0163-1829(98)07236-1]

I. INTRODUCTION

Carbon is a common impurity in Czochralski- or floating-zone-grown silicon.¹ It is initially incorporated as a substitutional defect (C_s) in concentrations as high as 10^{17} – 10^{18} cm⁻³. Upon 2 MeV electron irradiation, mobile silicon interstitials are created and react with C_s to form interstitial carbon (C_i).^{2,3} C_i also has enough mobility above room temperature to migrate and form defect complexes. Amongst these complexes, carbon-carbon pairs have been the most extensively studied by experimentalists. These pairs are commonly referred to interstitial-substitutional pairs (C_iC_s).

Song *et al.*⁴ have used a variety of experimental techniques in order to investigate structural, electronic, optical, and vibrational properties of these defects. Most interestingly, they have shown that carbon-carbon pairs display a bistability associated with two different structural configurations that are either stable or metastable depending on the charge state. They labeled these configurations *A* (stable in the +1 or -1 charge state) and *B* (stable in the neutral charge state). A complete configuration-coordinate energy surface was obtained for all three charge states, including energy-level positions and conversion barriers. Two gap states were found for each configuration: donor levels (0/+) at $E_v + 0.09$ eV (*A*) and $E_v + 0.05$ eV (*B*) and acceptor levels (-/0) at $E_c - 0.17$ eV (*A*) and $E_c - 0.11$ eV (*B*). Models were proposed for the *A* and *B* configurations based on electron paramagnetic resonance (EPR) measurements: a C-Si

split interstitial with a C_s bonded to the Si atom with C_{1h} symmetry for the *A* configuration and an unusual C_s -Si_{*i*}- C_s bridge configuration with the Si atom slightly off the bond center for the *B* configuration. The *B* configuration displayed C_{3v} symmetry along a $\langle 111 \rangle$ axis for $T > 15$ K and lower symmetry for lower temperatures, which is indicative a motional-averaged state. As will become clear later, the two configurations differ by a single bond switch, and they present intriguingly small differences in total energy (less than 0.05 eV for all charge states).⁵ In addition to that, an optical transition at 0.97 eV has been identified as arising from the *B* configuration⁴ and vibrational local-mode sidebands have been measured by photoluminescence.^{4,6,7} The local-mode structure and isotope splittings suggest decoupled vibrations at each of the carbon atoms, in apparent contradiction to the “symmetric” structure of the *B* configuration.

This rich variety of interesting properties is both attractive and challenging from a theoretical perspective. So far, a few theoretical calculations have been performed addressing particular aspects of this system. Tersoff⁸ has used empirical classical potentials to calculate the energies of several types of carbon defects in silicon, including carbon-carbon pairs. In agreement with experiment, he found both *A* and *B* configurations with very similar energies. A third low-energy metastable configuration was found (0.1 eV above *A* and *B*), corresponding to a C-C split interstitial that has not been detected experimentally. Burnard and DeLeo⁹ performed semiempirical electronic-structure calculations in clusters us-

ing several methods. Their results are somewhat parametrization dependent, but they also obtain the *A* and *B* configurations and the correct stability dependence on charge state, although the energy differences between stable and metastable configurations are much larger (0.4–0.6 eV) than experimental ones. They have also obtained vibrational frequencies somewhat higher than experiments. More recently, Leary *et al.*¹⁰ employed a local density functional (LDF) cluster method to investigate the geometry and vibrational spectrum of the isolated C_i and carbon-carbon pair. They obtain the *A* configuration as the ground state for all charge states, also with energy differences much larger than experiment (0.35 eV to 0.5 eV, depending on the charge state). However, they find the correct trend in charge state dependency: a configuration is more stable in charged configurations. Their calculated vibrational frequencies are in excellent agreement with experimental ones.

In this work we investigate a broad range of properties of carbon-carbon pairs in silicon by *ab initio* total-energy pseudopotential calculations. This approach has been successfully used to study the properties of the isolated carbon interstitial¹¹ and other carbon-related defects in silicon.¹² We focus our attention on the neutral charge state of the defect complex. Even though charge-state effects are extremely important (they drive the bistability of the defect), we will show that much can be learned from neutral-state investigation. We divide this paper as follows: In Sec. II, we summarize the technical aspects of our calculational method. Section III contains a detailed description of the *A* and *B* configurations of C_iC_s . In Sec. IV, we describe the electronic structure of the gap states for both configurations. Section V is devoted to the calculation of the energy barrier and mechanism for conversion from one configuration to the other. In Sec. VI, the vibrational properties of the defect are described. Finally, in Sec. VII we present our conclusions.

II. METHOD

We perform *ab initio* total-energy calculations based on the local-density approximation (LDA) of density-functional theory,¹³ with the exchange-correlation functional given by the Perdew-Zunger parametrization¹⁴ of Ceperley-Alder results.¹⁵ Separable norm-conserving nonlocal pseudopotentials with optimized convergence¹⁶ are used. This allows an energy cutoff of only 40 Ry for the plane-wave basis. A cubic supercell with 65 atoms (64 plus the interstitial) is used, which allows full relaxation up to second-nearest neighbors of the defect core (C-Si-C) according to Hellman-Feynman forces. Relaxation effects due to more distant neighbors are calculated using an empirical Keating potential.¹⁷ Reciprocal-space summations are performed either with the Γ point only or the special point $(\frac{1}{4}, \frac{1}{4}, \frac{1}{4})$, which unfolds into $3\vec{k}$ points when symmetry is lowered to C_{1h} . Electronic wave functions are obtained by the conjugate-gradients method.¹⁸

III. THE *A* AND *B* CONFIGURATIONS

Total-energy calculations performed as described above indicate the existence of the two (meta)stable configurations *A* and *B*. Figure 1 shows the fully relaxed atomic configura-

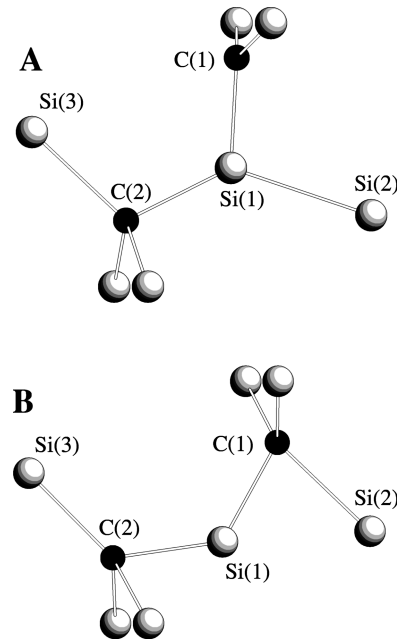


FIG. 1. Atomic configurations around the *A* and *B* carbon-carbon pairs. The plane of the figure is slightly rotated out of the (110) symmetry plane, so that out-of-plane atoms can be seen in perspective. Bond distances for *A*: C(1)-Si(1), 1.726 Å; C(2)-Si(1), 1.853 Å; Si(1)-Si(2), 2.342 Å; other C(1) bonds, 1.825 Å and 1.825 Å; other C(2) bonds, 1.984 Å, 1.984 Å, and 2.032 Å. Bond angles for *A*: C(1)-Si(1)-C(2), 119.5°; C(1)-Si(1)-Si(2), 105.4°; angles centered on C(1), 107.6°, 107.6°, and 141.6°. Bond distances for *B*: C(1)-Si(1), 1.833 Å; C(2)-Si(1), 1.805 Å; C(1)-Si(2), 2.083 Å; other C(1) bonds, 1.950 Å and 1.950 Å; other C(2) bonds, 2.026 Å, 2.026 Å, and 1.931 Å. Bond angles for *B*: C(1)-Si(1)-C(2), 127.3°; Si(1)-C(1)-Si(2), 75.7°.

tion around the defect core for both configurations. All bond lengths and some bond angles are shown in the figure caption. All geometrical parameters are in good agreement with the LDF cluster calculation of Leary *et al.*¹⁰ As proposed by experiments,⁴ configuration *A* is indeed similar to the atomic arrangement around a single C_i in silicon:¹¹ a C-Si $\langle 100 \rangle$ split-interstitial with threefold-coordinated C and Si interstitials slightly perturbed by a nearby substitutional carbon impurity. Configuration *B*, on the other hand, consists of an unusual twofold coordination for the central Si atom, which is accommodated between two substitutional carbons. As first noticed, to our knowledge, by Tersoff,⁸ both configurations are greatly stabilized by a partial cancelation of compressive and tensile stresses due to the interstitials (C-Si or Si) and substitutional carbon(s), respectively.

Our calculated energy of the *B* configuration is lower by 0.11 eV with respect to the *A* configuration for the neutral charge state.¹⁹ The experimental value is 0.02 eV. The difference (0.09 eV) is within the expected overall error introduced by the approximations involved in the calculation. It should be noticed that the near energy degeneracy of the two structures is accidental. It is due to a delicate interplay between chemical bonding and strain: The two configurations differ by a single bond switch where a Si-Si bond is replaced by a C-Si bond, which is lower in energy by 1.2 eV.²⁰ However, this energy difference is almost entirely compensated

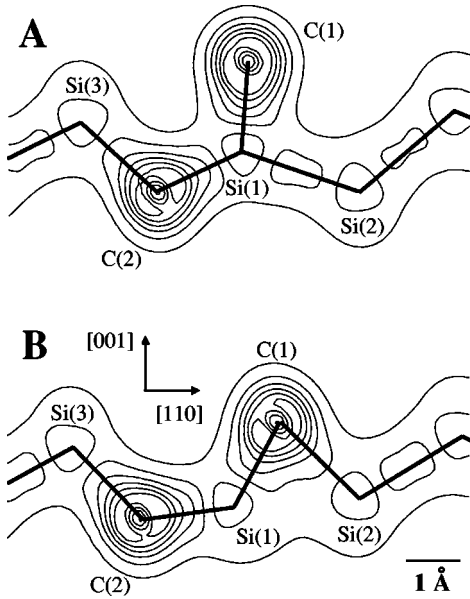


FIG. 2. Contour plots of the total valence electronic density in the mirror-symmetry plane for both *A* and *B* configurations. Contours vary from 0.25 to 1.50 in steps of 0.25 (units are electrons/Å³). Atom labels are the same as in Fig. 1. Thicker lines between atoms are a guidance to better visualize atomic positions.

for by the introduction of large strains in order to accommodate the Si interstitialcy.

Both configurations display the C_{1h} symmetry of a single mirror-symmetry (110) plane. This is consistent with the experimentally observed symmetry of configuration *A*. The configuration *B* has also C_{1h} symmetry, but the breaking of the Si-Si bond suggests that the central silicon atom can rotate almost freely around the C-C axis. Indeed, at temperatures above 15 K, as mentioned before, the *B* defect consists of a motional-averaged state with C_{3v} symmetry. In addition to this thermally induced “classical” rotation, a quantum rotation is observed even at very low temperatures,²¹ as a consequence of the tunneling of the central Si atom from one C_{1h} configuration to another. This tunneling is facilitated by the very small displacements (only $2\pi/6$ radians) necessary for rotating from one C_{1h} configuration to another. We have obtained the energy barrier for thermal rotation by calculating the energy of the expected saddle-point for rotation, an intermediate configuration with C_2 symmetry. We find a barrier of 0.07 eV for the thermally induced rotation, which is indeed very small but somewhat above the estimated experimental value of 0.01 eV.²¹

The bonding structure of both *A* and *B* configurations can be visualized in detail in Fig. 2, where the calculated valence electronic density is displayed. The plane of the figure is the mirror-symmetry plane. The carbon atoms can be easily pointed out in the figure due to the strong concentration of electrons around them, forming partly ionic bonds with the neighboring silicon. The silicon atoms show the usual depletion of (valence) charge on them and covalent bonding with each other. Going from *A* to *B*, one can clearly see that a Si-Si bond is broken and a C-Si bond is formed in its place.

IV. GAP STATES AND WAVE FUNCTIONS

In accordance to experimental results,⁴ we find two gap states near the band edges (donor and acceptor levels) for

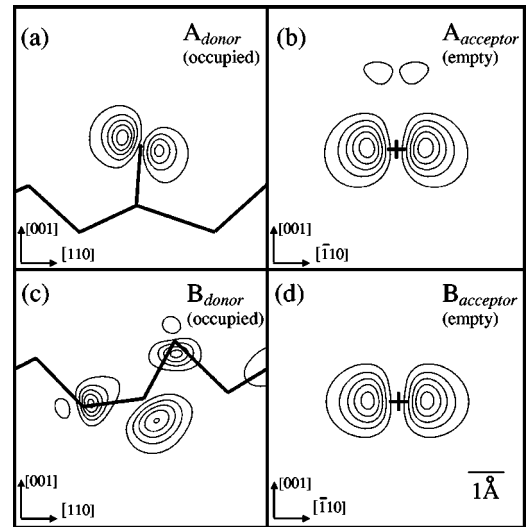


FIG. 3. Contour plots of gap-state electronic densities. Figures (a) and (c) correspond to the mirror-symmetry plane, and the thicker lines have the same meaning as in Fig. 2. Figures (b) and (d) correspond to a plane perpendicular to the symmetry plane which contains the central silicon atom (marked with a cross). (a) A_{donor} state, contours from 0.09 to 0.54 in steps of 0.25; (b) $A_{acceptor}$ state, contours from 0.02 to 0.12 in steps of 0.02; (c) B_{donor} state, contours from 0.012 to 0.072 in steps of 0.012; (d) $B_{acceptor}$ state, contours from 0.02 to 0.12 in steps of 0.02 (units are electrons/Å³).

both *A* and *B* configurations. Although Kohn-Sham eigenvalues cannot be quantitatively related to the excitation spectrum, it is possible to compare qualitative trends in the one-electron eigenstates with spin wave-function distributions inferred from EPR.⁴

For this purpose, we plot in Fig. 3 the electronic densities associated to each of the gap states. Figures 3(a) and 3(b) correspond, respectively, to donor and acceptor levels in the *A* configuration. The electronic signatures of both gap states are remarkably close to the states of isolated interstitial carbon in the split configuration,¹¹ as expected from the similarity of both structures. The lower gap state (A_{donor}) is a p -like state strongly localized on the carbon interstitial, whereas the upper gap state ($A_{acceptor}$) is a more extended p -like state on the silicon interstitial, with some contribution from nearby bonds. All of these features are in agreement with EPR results⁴ and they can be explained by the threefold coordination of both carbon and silicon in the C-Si split interstitial and by the higher electronegativity of carbon with respect to silicon.

As we have seen in the previous Section, the *B* configuration consists of a twofold-coordinated silicon interstitial between the carbon-carbon pair. Therefore we expect the two gap states to be primarily localized on the silicon. This is indeed what happens, as shown in Figs. 3(c) and 3(d). The $B_{acceptor}$ state [Fig. 3(d)] is a p -like state quite similar to the $A_{acceptor}$, but the B_{donor} state is substantially different from A_{donor} . It mainly consists of a sp^3 -like states on the silicon atom and on the neighboring carbons.

V. A TO B CONVERSION

We now calculate the energy barrier and pathway for conversion from the metastable *A* configuration to the stable *B*

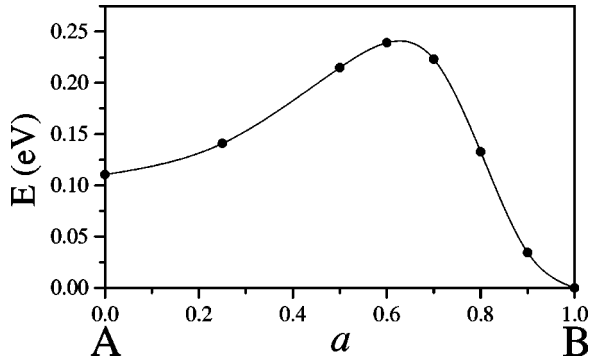


FIG. 4. Constrained total energy (in eV) as a function of the “conversion coordinate” a : Configurations A and B correspond to $a=0$ and $a=1$, respectively.

in the neutral charge state. Since there is no intermediate high-symmetry configuration from which a saddle-point could be inferred, we proceed by performing constrained total-energy calculations where the position of one of the atoms is restricted to planes perpendicular to a vector joining its initial (configuration A) and final (configuration B) positions.²² We choose C(1) to be the constrained atom (see Fig. 1) since it suffers the largest displacement during the conversion process. This procedure will define the minimum-energy pathway and, consequently, the energy barrier for conversion if one assumes the process to be adiabatic and in the absence of multiple valleys in the total-energy hypersurface. Deviations from adiabaticity will generally lead to higher barriers.²³

The results for the constrained total-energy calculations are shown in Fig. 4. In this figure, the “conversion coordinate” a running from 0 (A) to 1 (B) defines the plane that the C(1) is constrained to. The calculated activation energy for conversion from A to B in the neutral charge state is 0.13 eV, in good agreement with the experimental value of 0.16 eV.⁴ One can also notice that the barrier is very asymmetric: The A defect oscillates much more softly in the conversion coordinate than the B defect. This result is consistent with the large difference observed in measured prefactors for conversion time constants (9×10^{-12} s for A to B conversion and 4×10^{-13} s for B to A conversion).⁴ In Fig. 5 we illustrate the minimum-energy pathway by plotting snapshots of the ionic positions during the conversion process. As expected, the atoms in the defect core remain on the symmetry plane all along the conversion pathway.

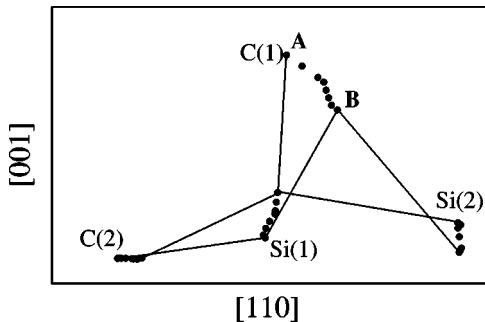


FIG. 5. Ionic positions in the mirror-symmetry plane illustrating the conversion pathway.

TABLE I. Vibrational frequencies (in cm^{-1}) and isotope shifts of local modes for the B configuration. Experimental frequencies are in parentheses.

Symm.	$^{12}\text{C}-^{12}\text{C}$	$^{12}\text{C}-^{13}\text{C}$	$^{13}\text{C}-^{12}\text{C}$	$^{13}\text{C}-^{13}\text{C}$
A	841.1	822.6	838.8	819.3
A	715.7	710.8	694.6	690.7
B	643.4	643.4	624.1	624.1
A	567.0	552.4	566.0	551.3
	(579.5)		(578.9)	(564.6)
B	513.8	506.5	513.8	506.4
A	502.8	501.7	499.1	499.0
	(543.0)	(542.9)		(532.9)

VI. LOCAL VIBRATIONAL MODES

To determine the local vibrational modes for the A and B configurations we calculate the matrix of force constants using a finite-difference approach. The matrix element $\Phi_{i\alpha,j\beta}$ is approximated by $-\delta F_{j\beta}/\delta R_{i,\alpha}$, where $\delta F_{j\beta}$ is the calculated force on atom j , direction β , for a small displacement $\delta R_{i,\alpha}$ on atom i along direction α . Displacements are executed on the atoms around the defect core (including the first-neighbor shell). Bulk Si force constants, also calculated *ab initio*, are used for the matrix elements of the outer shells.

We first present our results for the B defect, since this is the case for which both photoluminescence^{4,6,7} (PL) and theoretical¹⁰ results are available for comparison. Table I shows our calculated along with experimental vibrational frequencies of the local modes, including isotope splittings. We also plot, in Fig. 6, the phonon eigenstates for the modes that transform as the A representation of the point group (in-plane vibrations of the C-Si-C defect core). To analyze the modes, it is instructive to recall the vibrations of an isolated C-Si-C molecule. The highest- and second-highest frequency modes [841.1 cm^{-1} and 715.7 cm^{-1} , Fig. 6(a) and 6(b)] are reminiscent of the antisymmetric stretch and breathing modes, respectively, of the isolated molecule. In the molecule, PL sidebands due to the antisymmetric mode would be forbidden. Indeed, this mode is not observed experimentally, although symmetry breaking due to the crystal field would make it weakly allowed. The breathing mode, however, is also not observed in PL as it should by symmetry considerations and it has been suggested¹⁰ that this may happen be-

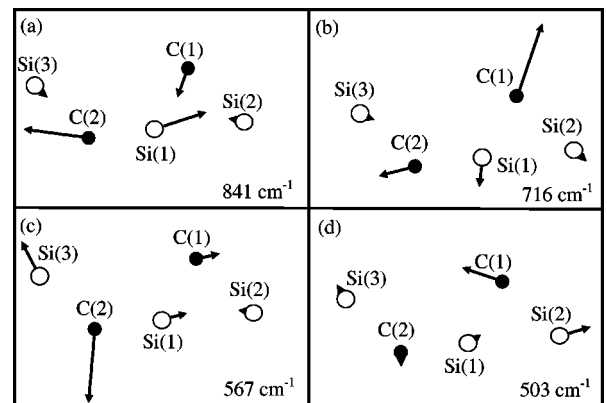


FIG. 6. In-plane local modes for the B configuration.

TABLE II. Vibrational frequencies (in cm^{-1}) and isotope shifts of local modes for the A configuration.

Symm.	$^{12}\text{C}-^{12}\text{C}$	$^{12}\text{C}-^{13}\text{C}$	$^{13}\text{C}-^{12}\text{C}$	$^{13}\text{C}-^{13}\text{C}$
A	889.9	889.6	863.1	862.5
B	874.1	874.1	847.2	847.2
A	721.8	701.6	720.3	700.3
A	567.5	550.6	567.3	550.4
B	557.1	540.9	557.1	540.9

cause of short lifetimes due to B to A conversion. Going to lower energies, one finds two modes (643.4 cm^{-1} and 513.8 cm^{-1}) that transform as the B representation, corresponding to decoupled out-of-plane vibrations of each of the carbons (not plotted in Fig. 6). Between them, there is a mode with A symmetry [567.0 cm^{-1} , Fig. 6(c)], reminiscent of the symmetric stretch mode of the isolated molecule, but with a stronger component in $C(2)$ than in $C(1)$. In fact, this mode can be seen as a vibration of $C(2)$ against its neighbors. There is a similar mode for $C(1)$ at 502.8 cm^{-1} [Fig. 6(d)]. These two modes are the ones that fit more closely the experimentally observed frequencies and isotope splittings.¹⁰ The largest discrepancy between theory and experiment is around 7% on the 502.8 cm^{-1} mode. Discrepancies of this order in elastic properties are not unreasonable in this type of calculation.

An intriguing picture emerges from these results: an inequivalence between the two carbon atoms. This can be seen in the mode patterns, in the splitting between the experimentally observed modes and in the isotope splittings of each mode. This inequivalence was once seen as a puzzle,⁴ since the B configuration was understood as being composed of two equivalent atoms with an interstitial Si between them. Our results show this is not so, and complete equivalence between the carbons is only recovered at higher temperatures in the motional-averaged configuration. The inequivalence comes from the fact that $\text{Si}(1)$ is closer to $\text{Si}(2)$ than to $\text{Si}(3)$. This makes the $C(1)\text{-Si}(2)$ bond weaker than the $C(2)\text{-Si}(3)$ bond. Indeed, the bond lengths are 2.083 \AA and 1.931 \AA , respectively (see Fig. 1). Therefore, vibrations at $C(1)$ tend to be softer than corresponding ones at $C(2)$. This decoupling of $C(1)$ and $C(2)$ modes was also observed by Leary *et al.*¹⁰

Calculated vibrational frequencies and isotope shifts for the A defect are shown in Table II. As discussed before, the structure of the carbon-carbon pair in configuration A is similar to the isolated C_i , slightly perturbed by the presence of the substitutional carbon. It is therefore expected that the inequivalence between carbon atoms is even more accentuated in this case, resulting in “ C_i -like” and “ C_s -like” vibrations. This can be deduced from the isotope shifts shown in Table II: The two higher-frequency modes are strongly localized on $C(1)$ (C_i) and the three lower-frequency ones are localized on $C(2)$ (C_s).

Let us begin by analyzing the three C_s -like modes. An isolated substitutional carbon with full T_d symmetry would display a threefold degenerate localized vibrational mode at 605 cm^{-1} .²⁴ Symmetry lowering to C_{1h} caused by the pair formation splits this mode into two A -symmetry modes [in-plane vibrations of $C(2)$] at 721.8 cm^{-1} and 567.5 cm^{-1} and one B -symmetry mode (out of plane) at 557.1 cm^{-1} . The

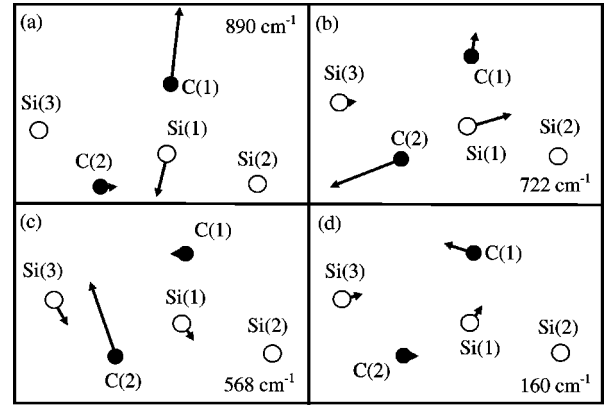


FIG. 7. In-plane local modes for the A configuration.

eigenvectors corresponding to the two in-plane modes are shown in Figs. 7(b) and 7(c).

The two higher-frequency modes at 889.9 cm^{-1} and 874.1 cm^{-1} correspond to in-plane and out-of-plane vibrations of C_i . Analysis of these modes provides insightful information about the isolated C_i vibrations. The vibrational spectrum of isolated C_i remained a puzzle for a long time since it consists of two nearly degenerate lines at 921.0 cm^{-1} and 930.3 cm^{-1} with a 2:1 intensity ratio, which suggested a $\langle 111 \rangle C_{3v}$ symmetry for the defect.³ Recent infrared-absorption measurements under uniaxial stress confirm the assignment of these lines to the neutral C_i but unambiguously show that the symmetry is C_{2v} ,²⁵ therefore suggesting that the near degeneracy between the modes and their 2:1 intensity ratio are accidental effects.

In Fig. 7(a) we plot the in-plane C_i vibrational eigenvector. The out-of-plane mode (not plotted) consists essentially of vibrations of the C_i against its out-of-plane neighbors. In addition to these high-frequency localized modes, a low-frequency C_i mode corresponding to vibrations roughly perpendicular to all its C-Si bonds is expected to occur.⁹ We find this mode as a broad resonance around 160 cm^{-1} and we plot it in Fig. 7(d).

VII. CONCLUSIONS

We have studied structural, electronic, and vibrational properties of neutral carbon-carbon pairs in silicon by *ab initio* total-energy calculations. Our results confirm the existence of the two experimentally observed (meta)stable configurations (A and B) of the defect pair. As described above, the A configuration is similar to the isolated C_i , but the B configurations presents a somewhat unusual twofold-coordinated silicon in a bridge site between the two carbons. The two configurations differ by a single bond switch and they are nearly energy degenerate due to an accidental cancellation of chemical bonding and strain energies. We calculate the energy difference between A and B configurations (0.11 eV), the activation energy for the thermally induced rotation of the central silicon atom in the B configuration (0.07 eV) and the activation energy for A to B conversion (0.13 eV). The experimental values are 0.02 eV , $\sim 0.01 \text{ eV}$, and 0.16 eV , respectively. The agreement is fair, given that the overall uncertainty of the calculations due to the approximations involved (LDA, supercell, k -space sampling) is

about 0.1 eV, making it hard to describe such small energy differences.

Nevertheless, a good understanding of many physical aspects of this system is obtained. Two gap states are found for each configuration, with wave functions localized on the under coordinated atoms of the defect complex in each case. The A to B conversion barrier and pathway has been described. A quantitative analysis of the local vibrational modes of each configuration is presented and the observed inequivalence of the carbon atoms in the B configuration is explained. Finally, the local modes for the A configuration are predicted: they consist of C_i -like and C_s -like vibrations,

and the C_i -like modes present the same twofold near degeneracy of the isolated C_i , which was interpreted as an accidental effect.

ACKNOWLEDGMENTS

This work was partially supported by Conselho Nacional de Desenvolvimento Científico e Tecnológico (CNPq). The use of computational facilities at Núcleo de Atendimento em Computação de Alto Desempenho (NACAD-COPPE/UFRJ) is also acknowledged.

-
- ¹See, for example, *Oxygen, Carbon, Hydrogen, and Nitrogen in Crystalline Silicon*, edited by J. C. Mikkelsen, Jr. *et al.*, MRS Symposia Proceedings No. 59 (Materials Research Society, Pittsburgh, 1986).
- ²G. D. Watkins and K. L. Brower, *Phys. Rev. Lett.* **36**, 1329 (1976).
- ³A. R. Bean and R. C. Newman, *Solid State Commun.* **8**, 175 (1970).
- ⁴L. W. Song, X. D. Zhan, B. W. Benson, and G. D. Watkins, *Phys. Rev. B* **42**, 5765 (1990), and references therein.
- ⁵The total energy differences $E_B - E_A$ were measured to be -0.04 eV, 0.02 eV, and -0.05 eV for the positive, neutral, and negative charge states, respectively. The details on the experimental techniques can be found in Ref. 4.
- ⁶G. Davies, E. C. Lightowlers, and M. do Carmo, *J. Phys. C* **16**, 5503 (1983).
- ⁷G. Davies and R. C. Newman, in *Handbook on Semiconductors* Vol. 3, edited by S. Mahajan (Elsevier, Amsterdam, 1994), p. 1557.
- ⁸J. Tersoff, *Phys. Rev. Lett.* **64**, 1757 (1990).
- ⁹M. J. Burnard and G. G. DeLeo, *Phys. Rev. B* **47**, 10 217 (1993).
- ¹⁰P. Leary, R. Jones, S. Öberg, and V. J. B. Torres, *Phys. Rev. B* **55**, 2188 (1997); R. Jones, S. Öberg, P. Leary, and V. Torres, *Mater. Sci. Forum* **196–201**, 785 (1995).
- ¹¹R. B. Capaz, A. Dal Pino, Jr., and J. D. Joannopoulos, *Phys. Rev. B* **50**, 7439 (1994).
- ¹²A. Dal Pino, Jr., A. M. Rappe, and J. D. Joannopoulos, *Phys. Rev. B* **47**, 12 554 (1993).
- ¹³P. Hohenberg and W. Kohn, *Phys. Rev.* **136**, B864 (1964); W. Kohn and L. J. Sham, *Phys. Rev.* **140**, A1133 (1965).
- ¹⁴J. P. Perdew and A. Zunger, *Phys. Rev. B* **23**, 5048 (1984).
- ¹⁵D. M. Ceperley and B. J. Alder, *Phys. Rev. Lett.* **45**, 566 (1980).
- ¹⁶A. M. Rappe, K. M. Rabe, E. Kaxiras, and J. D. Joannopoulos, *Phys. Rev. B* **41**, 1227 (1990).
- ¹⁷P. N. Keating, *Phys. Rev.* **145**, 637 (1966).
- ¹⁸M. C. Payne, M. P. Teter, D. C. Allan, T. A. Arias, and J. D. Joannopoulos, *Rev. Mod. Phys.* **64**, 1045 (1992).
- ¹⁹The Keating relaxation energies are 0.30 eV for the B configuration and 0.25 eV for the A configuration. Therefore it increases the energy difference $E_A - E_B$ by 0.05 eV. This would be a minor correction in other systems, but in this case it is relevant because of the small energy differences.
- ²⁰L. Pauling, *The Nature of the Chemical Bond and the Structure of Molecules and Crystals*, 3rd ed. (Cornell University Press, Ithaca, NY, 1960), p. 85.
- ²¹K. P. O'Donnell, K. M. Lee, and G. D. Watkins, *Physica B & C* **116B**, 258 (1983).
- ²²A. Dal Pino, Jr., M. Needels, and J. D. Joannopoulos, *Phys. Rev. B* **45**, 3304 (1992).
- ²³M. Needels, J. D. Joannopoulos, Y. Bar-Yam, S. T. Pantelides, and R. H. Wolfe, in *Defects on Materials*, edited by P. D. Bristowe, J. E. Epperson, J. E. Griffith, and Z. Liliental-Weber, MRS Symposia Proceedings No. 209 (Materials Research Society, Pittsburgh, 1991), p. 102.
- ²⁴R. C. Newman and R. S. Smith, *J. Phys. Chem. Solids* **30**, 1492 (1969).
- ²⁵J. F. Zheng, M. Stavola, and G. D. Watkins, in *22nd International Conference on The Physics of Semiconductors*, edited by D. J. Lockwood (World Scientific, Singapore, 1994), p. 2363.